Three-dimensional reconstruction by holographic LEED: Proper identification of the reference wave

D. K. Saldin
Department of Physics and Laboratory for Surface Studies, University of Wisconsin-Milwaukee, Milwaukee, Wisconsin 53211 and Condensed Matter Theory Group, Blackett Laboratory, Imperial College, London SW7 2BZ, United Kingdom

X. Chen
Department of Physics and Laboratory for Surface Studies, University of Wisconsin-Milwaukee, Milwaukee, Wisconsin 53211
(Received 18 November 1994; revised manuscript received 25 April 1995)

It is shown in this paper that the proper identification of the reference wave is the key to the successful reconstruction of a three-dimensional image of the configuration of an atomic adsorption site from a set of diffuse low-energy electron diffraction (DLEED) patterns of different electron energies, but the same direction of incidence of the electron beam. We develop a reconstruction algorithm based on this idea, and demonstrate its effectiveness by application to a set of calculated DLEED patterns. A powerful feature of our algorithm is that it also filters out any residual effects on the diffraction patterns of long-range order amongst the adsorbates, thus enabling the application of holographic LEED to disordered adsorbates of much higher coverage.

I. INTRODUCTION

Low-energy electron diffraction[1] (LEED) plays the same role in surface crystallography that x-ray diffraction does in the crystallography of bulk materials. However, one of the very properties that enables low-energy electrons to be such useful probes of surfaces, namely, their strong scattering by atoms, turns out to be an equally strong obstacle to the development of *direct* methods[2,3] for surface structure determination, due to the multiple-scattering problem.

Szöke[4] and Barton[5] have proposed holographic[6] methods of structure determination in photoelectron diffraction, where the source of electrons is not some external gun, but atomic cores within the sample. Saldin and De Andres[7] pointed out that similar ideas may be applied to the diffuse LEED (or DLEED) patterns formed from the diffraction of low-energy electrons from a surface containing disordered adsorbates. Saldin and DeAndres[7] illustrated their theory with reconstructions, from several simulated DLEED patterns, of the positions of near-neighbor substrate atoms relative to oxygen adsorbate atoms in hollow sites on a Ni(001) surface. Recognizing that the fractional-order spots on LEED patterns from an ordered array of adsorbates on a surface sample the DLEED pattern from a corresponding disordered adsorbate layer, Heinz and co-workers[8] and Hu and King[9] applied similar holographic techniques to such conventional LEED patterns.

It was also recognized early[7,10] that the quality and reliability of the reconstructed images may be improved by simultaneously using data from diffraction patterns of electrons of several different energies. Reconstruction algorithms with energy-dependent phase factors[10,11] have also been used to recover three-dimensional atomic geometries of clean and adsorbate-covered surfaces from experimental photoelectron diffraction patterns.[12] There have been parallel developments in the theory of holographic LEED,[9,13] demonstrated recently with DLEED experimental data.[14]

In the most recent work on holographic LEED,[9,13–15] the reference wave has been defined as that part of the incident electron beam (assumed to be approximated by a plane wave) forward scattered by an adsorbate. At common LEED energies of the order of hundreds of eV, atomic scattering factors for electrons are highly forward peaked. The resulting holographic reference wave is very anisotropic, a circumstance not ideal for the reconstruction of good quality three-dimensional images.[16] The above authors[9,13,14] found that, for a given direction of incidence of the electron beam, only the substrate atoms close to the forward-scattering direction were reconstructed well. In order to generate a satisfactory *three-dimensional* image, they used information from several sets of multienergy diffraction patterns, each set from electron beams with different directions of incidence. If the directions from the adsorbate in which near-neighbor substrate atoms are found is not known beforehand, as in the case of a truly unknown structure, the number of LEED patterns that must be measured may increase by even a further order of magnitude.

In this paper we return to the definition of the reference wave of the original paper by Saldin and De Andres,[7] namely, as the wave that leaves the adsorbate for the last time *after* all prior multiple scattering between adsorbate and substrate.[17,18] We will show that, instead of the experimentally difficult and time-consuming process of using incident electron beams from different directions, the anisotropy of the reference waves may be compensated for by a very simple mathematical estimation of that anisotropy. Such an algorithm is somewhat analogous to the scattered-wave included Fourier transform[19,20] (SWIFT) method of correcting for the anisotropy of the *object* wave in photoelectron diffraction. In

0163-1829/95/52(4)/2941(8)/$06.00

diffuse LEED, of course, where the adsorbates act as beam splitters of some external electron beam, the reference wave is a *scattered* wave. We find that use of our algorithm enables the reconstruction of high-quality images of the local environments of adsorbate atoms from a set of multienergy DLEED patterns due to external electron beams along a *single* direction of incidence, thus requiring no prior knowledge whatsoever of substrate atom directions, and reducing substantially the required set of experimental data.

II. THE HOLOGRAPHIC VIEW OF DIFFUSE LEED

Pendry and Saldin[17] have given a general theory of diffuse LEED. They pointed out that diffuse LEED amplitudes may be calculated on a three-step model. Evaluated in step 1 is the sum of the amplitudes of propagation, over all possible paths, of an electron from its distant source to its first encounter with an adsorbate. In step 2, the total amplitude of all propagation paths of an electron between its first and last encounter with the adsorbate is calculated, and in step 3 the total propagation amplitude from its last encounter with the adsorbate to the detector is computed. The multiple scattering in step 2 may be evaluated in a spherical-wave basis by considering a cluster of atoms around the adsorbate, and by evaluating the reflection matrix of that cluster.[21] However, DLEED calculations[22] have shown that, under typical electron energies in a LEED experiment, the backscattering amplitudes from the cluster are usually quite negligible, and that, in practice, step 2 may be omitted altogether. We follow this practice in the calculations reported in this paper.

The propagation amplitudes in step 1 may be evaluated very conveniently, using the formalism and computational machinery of conventional LEED, according to which a plane wave incident with unit (real) amplitude at a conventional origin, $\mathbf{r}_o$, immediately above a crystal surface, generates a set of Bragg waves, reflected back from the surface, and of (complex) amplitudes $R_{o\mathbf{g}}$ at the same origin. The reflection amplitudes $R_{o\mathbf{g}}$ are calculated by conventional LEED programs.[1] The resulting total electron amplitude at some arbitrary position $\mathbf{r}_a$ is therefore

$$e^{i\mathbf{K}_o^+\cdot(\mathbf{r}_a-\mathbf{r}_o)}+\sum_{\mathbf{g}}R_{o\mathbf{g}}(\mathbf{k}_{\parallel}^{\mathrm{inc}})e^{i\mathbf{K}_{\mathbf{g}}^-\cdot(\mathbf{r}_a-\mathbf{r}_o)} . \tag{1}$$

In the above expression, the wave vectors $\mathbf{K}_{\mathbf{g}}^{\pm}$ are defined in terms of their components parallel and perpendicular to the surface by

$$\mathbf{K}_{\mathbf{g}}^{\pm}=(\mathbf{k}_{\parallel}^{\mathrm{inc}}+\mathbf{g},K_{\mathbf{g}\perp}^{\pm}) , \tag{2}$$

where $\mathbf{k}_{\parallel}^{\mathrm{inc}}$ is the parallel wave-vector component of the incident beam, $\mathbf{g}$ is a reciprocal-lattice vector, and the superscripts $\pm$ indicate whether the wave vectors are directed into or out of the surface, respectively.[17] The perpendicular components of $\mathbf{K}_{\mathbf{g}}^{\pm}$ are

$$K_{\mathbf{g}\perp}^{\pm}=\pm(\kappa^2-|\mathbf{k}_{\parallel}^{\mathrm{inc}}+\mathbf{g}|^2)^{1/2} , \tag{3}$$

where the magnitudes κ of the wave vectors inside the crystal are given by

$$\tfrac{1}{2}\kappa^2=E-V_o \tag{4}$$

(in hartree atomic units), E being the total energy of the electron, and V_o the potential-energy step at the surface, generally a negative quantity.

If $\mathbf{r}_a$ is identified with the position of an adsorbate on the surface, expression (1) can be regarded as a sum of plane-wave amplitudes incident on that adsorbate. Each of the component plane waves gives rise to a scattered wave, and the total amplitude at a position $\mathbf{r}$ relative to the adsorbate, due to the sum of all the scattered waves, may be written in the form

$$A(\hat{\mathbf{r}})e^{ikr}/r , \tag{5}$$

where $\hat{\mathbf{r}}$ specifies the direction of $\mathbf{r}$, with

$$A(\hat{\mathbf{r}})=e^{i\mathbf{K}_o^+\cdot(\mathbf{r}_a-\mathbf{r}_o)}f_a(\mathbf{K}_o^+\cdot\hat{\mathbf{r}}) +\sum_{\mathbf{g}}R_{o\mathbf{g}}(\mathbf{k}_{\parallel}^{\mathrm{inc}})e^{i\mathbf{K}_{\mathbf{g}}^-\cdot(\mathbf{r}_a-\mathbf{r}_o)}f_a(\mathbf{K}_{\mathbf{g}}^-\cdot\hat{\mathbf{r}}) \tag{6}$$

and

$$f_a(\mathbf{k}_1\cdot\hat{\mathbf{k}}_2)=\frac{1}{k_1}\sum_l(2l+1)\sin\{\delta_l(k_1)\} \times\exp\{i\delta_l(k_1)\}P_l(\hat{\mathbf{k}}_1\cdot\hat{\mathbf{k}}_2) \tag{7}$$

is the scattering factor of the adsorbate, describing the elastic scattering of an electron of wave vector $\mathbf{k}_1$ into a direction specified by the unit vector $\hat{\mathbf{k}}_2$. The quantity $\delta_l(k_1)$ is the atomic phase shift of angular momentum quantum number l of an electron of wave number k_1, and $P_l[\cos(\theta)]$ is a Legendre polynomial, where θ is the angle of scattering.

A DLEED pattern is formed from the subsequent propagation and scattering of the wave (5), which is step 3 of the three-step model of DLEED.[17] It was this step that was described in holographic terms in the original paper of Saldin and De Andres.[7] In such a picture, Eq. (5) represents a reference wave R, originating at the adsorbate, and the object wave O is identified with the extra wavelets generated by the scattering of this reference wave by the atoms in the vicinity of the adsorbate. In the direction corresponding to a detected wave vector $\mathbf{k}$, the kinematic (or single-scattering) estimate of the object waves is then

$$\sum_j A(\hat{\mathbf{r}}_j)\frac{e^{ikr_j}}{r_j}f_s(\hat{\mathbf{r}}_j\cdot\mathbf{k})\frac{e^{ik|\mathbf{r}-\mathbf{r}_j|}}{|\mathbf{r}-\mathbf{r}_j|} , \tag{8}$$

where $\mathbf{r}_j$ is the position of a nearby atomic scatterer, and $f_s(\hat{\mathbf{k}}_3\cdot\mathbf{k}_4)$ is the scattering factor of a substrate atom, defined in analogy with (7), describing the scattering of an electron incident from a direction $\hat{\mathbf{k}}_3$ into a state specified by the wave vector $\mathbf{k}_4$.

Apart from some unimportant common factors, the total DLEED amplitude at a point on a far-field diffraction pattern corresponding to the detected wave vector $\mathbf{k}$ may be found by combining (5) and (8) and writing

$$R(\mathbf{k})+O(\mathbf{k}) , \tag{9}$$

where

$$R(\mathbf{k})=A(\hat{\mathbf{k}}) \tag{10}$$

and

$$O(\mathbf{k})=\sum_j A(\hat{\mathbf{r}}_j)\frac{f_s(\hat{\mathbf{r}}_j\cdot\mathbf{k})}{r_j}e^{i(kr_j-\mathbf{k}\cdot\mathbf{r}_j)} . \tag{11}$$

The intensity of the DLEED pattern therefore takes the form

$$H(\mathbf{k})=|R(\mathbf{k})+O(\mathbf{k})|^2=|R(\mathbf{k})|^2+R(\mathbf{k})O^*(\mathbf{k})+R^*(\mathbf{k})O(\mathbf{k})+|O(\mathbf{k})|^2$$
$$=|A(\hat{\mathbf{k}})|^2+\left[A(\hat{\mathbf{k}})^*\sum_j A(\hat{\mathbf{r}}_j)\frac{f_s(\hat{\mathbf{r}}_j\cdot\mathbf{k})}{r_j}e^{i(kr_j-\mathbf{k}\cdot\mathbf{r}_j)}+\text{c.c.}\right]+\cdots , \tag{12}$$

where c.c. denotes complex conjugation, and the $|O(\mathbf{k})|^2$ term is not written explicitly.

The expression (12) gives an explicit dependence of the intensity $H(\mathbf{k})$ of a DLEED pattern on the positions $\mathbf{r}_j$ of the scatterers relative to the adsorbate. In Sec. III we examine how to construct an appropriate algorithm to recover a fully *three-dimensional* picture of the nearest scatterers to the adsorbate from a set of DLEED patterns of different electron energies, but with *a single direction of incidence* of the external electron beam.

III. AN ACCURATE AND PRACTICAL RECONSTRUCTION ALGORITHM FOR DLEED

The right-hand side of (12) suggests that the rapidly varying exponential terms within the square brackets give rise to a set of interference fringes in $H(\mathbf{k})$, whose periodicity depends on the position vectors $\mathbf{r}_j$. Holographic reconstruction algorithms seek to recover those position vectors from their corresponding interference fringes by Fourier transform methods.

Barton's suggestion[10] for such an algorithm in the analogous case of photoelectron diffraction was

$$B(\mathbf{r})=\int\int\int H(\mathbf{k})e^{-i(kr-\mathbf{k}\cdot\mathbf{r})}d^3k , \tag{13}$$

where the triple integral indicates integration over all three Cartesian components of $\mathbf{k}$, it being understood that the integrals be performed over only that domain of $\mathbf{k}$ over which values of the function $H(\mathbf{k})$ are known. Such an algorithm would be effective in DLEED also, if the coefficient of the exponential displayed in (12) were slowly varying with $\mathbf{k}$. Then, substituting (12) into (13), one could argue that stationary-phase conditions from the exponential terms would tend to occur only for values of $\mathbf{r}\simeq\mathbf{r}_j$, and hence that a plot of $|B(\mathbf{r})|^2$ would reconstruct the real-space distribution of scattering atoms around the adsorbate.

A closer examination of the first term within the square brackets in (12) suggests that such a simple algorithm is likely to run into difficulties in DLEED. There is no guarantee that the terms multiplying the exponentials in (12) that depend on $\mathbf{k}$ will, in fact, be slowly varying over the whole of the domain of integration of $\mathbf{k}$ (which will include variations of both magnitude and direction of $\mathbf{k}$).

Also, the terms that depend on $\mathbf{r}_j$ may tend to enhance the amplitudes of the interference fringes due to scatterers in particular directions or distances from the adsorbate. For instance, the appearance of the distance r_j in the denominator of the coefficients of the exponentials in (12) implies that the holographic fringes due to more distant scatterers have lower amplitudes. The term $A(\hat{\mathbf{r}}_j)$ will tend to enhance the interference fringes due to scatterers in directions in which this quantity has a large amplitude. An examination of (6) suggests that $|A(\hat{\mathbf{r}})|$ will be largest in the direction of the incident wave vector $\mathbf{K}_o^+$ since the atomic scattering factor f_a would be expected to be highly forward peaked at usual LEED energies [we will argue below that the second term on the right-hand side of (6) would be expected to be much more *isotropic*].

An improved reconstruction scheme is suggested the SWIFT algorithm[19,20] of photoelectron diffraction: consider the replacement of (13) by

$$B(\mathbf{r})=\int\int\int K(\mathbf{k},\mathbf{r})H(\mathbf{k})e^{-i(kr-\mathbf{k}\cdot\mathbf{r})}d^3k , \tag{14}$$

where the kernel K is formed by the inverse of the coefficients of each of the exponential terms in (12) with the general position vector $\mathbf{r}$ replacing the unknown atom positions $\mathbf{r}_j$. In this case

$$K(\mathbf{k},\mathbf{r})=\left[A(\hat{\mathbf{k}})A(\hat{\mathbf{r}})\frac{f_s(\hat{\mathbf{r}}\cdot\mathbf{k})}{r}\right]^{-1} . \tag{15}$$

This kernel cancels the coefficients of the exponentials in (12) when $\mathbf{r}=\mathbf{r}_j$ to give a good stationary-phase condition in the integral over $\mathbf{k}$ for those real-space points, but not elsewhere, thus enabling a good reconstruction of the nearby atom scatterer positions.

A problem that arises in DLEED is that the coefficients A in (15) themselves depend on the quantity $(\mathbf{r}_a-\mathbf{r}_o)$, which specifies the position of the adsorbate relative to the substrate, the very geometrical quantity sought in DLEED. Although, in principle, this quantity may be related to the same vectors $\mathbf{r}_j$ that appear explicitly in (12) (if the substrate is assumed to be not reconstructed by the adsorption process), and thus be used to construct a kernel $K(\mathbf{k},\mathbf{r})$ that contains the substrate backscattering amplitudes R_{og}, we will show that simple physical arguments will enable the construction of a much simpler kernel, which makes no assumption *a priori* about the state of local substrate reconstruction around the adsorbate.

Consider replacing (14) by

$$B(\mathbf{r})=\int\int\left[\int K(k_\perp,\mathbf{k}_\parallel;\mathbf{r})\chi(k_\perp,\mathbf{k}_\parallel)e^{-i(kr-k_\perp z)}dk_\perp\right]\times e^{i\mathbf{k}_\parallel\cdot\mathbf{r}_\parallel}d^2\mathbf{k}_\parallel\ , \tag{16}$$

where $\mathbf{k}_\parallel$ and $k_\perp$ are the components of $\mathbf{k}$ parallel and perpendicular to the surface, z is the component of $\mathbf{r}$ perpendicular to the surface,

$$\chi(k_\perp,\mathbf{k}_\parallel)=\frac{H(k_\perp,\mathbf{k}_\parallel)-H_{\rm av}(\mathbf{k}_\parallel)}{H_{\rm av}(\mathbf{k}_\parallel)}\ , \tag{17}$$

and

$$H_{\rm av}(\mathbf{k}_\parallel)=\frac{\int H(k_\perp,\mathbf{k}_\parallel)dk_\perp}{\int dk_\perp}\ . \tag{18}$$

In Eq. (16) we have factorized the three-dimensional integral over the vector $\mathbf{k}$ in (14) into a one-dimensional integral over $k_\perp$ and a two-dimensional one over $\mathbf{k}_\parallel$. In addition, we have replaced the DLEED intensity H in the integrand by the function χ, which enhances the contrast of the oscillations in $H(\mathbf{k}_\parallel)$, without affecting their periodicities. A practical advantage of replacing H by χ in the integrand of (17) is that the latter function would also tend to filter out unwanted smooth background contributions to a measured DLEED pattern from, e.g., thermal diffuse scattering or lattice defects. Another important practical reason for replacing H by χ in the reconstruction algorithm (16) will be pointed out in Sec. V.

A careful examination of Eq. (12) reveals that, for a given $\mathbf{k}_\parallel$, $H(\mathbf{k})$ oscillates with $k_\perp$ mainly due to the terms in the square brackets on the right-hand side of (12). Therefore, approximating $H_{\rm av}(\mathbf{k}_\parallel)$ by the nonoscillatory term $|A(\hat{\mathbf{k}})|^2$, and substituting (12) into (17), it may be argued that

$$\chi(k_\perp,\mathbf{k}_\parallel)\simeq\sum_j\left[\frac{A(\hat{\mathbf{r}}_j)}{A(\hat{\mathbf{k}})}\frac{f_s(\hat{\mathbf{r}}_j\cdot\mathbf{k})}{r_j}\times e^{i(kr_j-\mathbf{k}\cdot\mathbf{r}_j)}+\text{c.c.}\right]+\cdots\ . \tag{19}$$

The appropriate SWIFT kernel in this case may thus be taken as

$$K(k_\perp,\mathbf{k}_\parallel;\mathbf{r})=\left[\frac{A(\hat{\mathbf{r}})}{A(\hat{\mathbf{k}})}\frac{f_s^-(\hat{\mathbf{r}}\cdot\mathbf{k})}{r}\right]^{-1}\ . \tag{20}$$

Substituting the explicit expressions for the amplitudes A from (6), this may be reexpressed as

$$K(k_\perp,\mathbf{k}_\parallel;\mathbf{r})=\left[\{f_a^+(\mathbf{K}_o^+\cdot\hat{\mathbf{r}})+C\}\frac{f_s^-(\hat{\mathbf{r}}\cdot\mathbf{k})}{Dr}\right]^{-1}\ , \tag{21}$$

where

$$C=\sum_{\mathbf{g}}R_{o\mathbf{g}}(\mathbf{k}_\parallel^{\rm inc})e^{i(\mathbf{K}_\mathbf{g}^--\mathbf{K}_o^+)\cdot(\mathbf{r}_a-\mathbf{r}_o)}f_a^-(\mathbf{K}_\mathbf{g}^-\cdot\hat{\mathbf{r}}) \tag{22}$$

and

$$D=f_a^-(\mathbf{K}_o^+\cdot\hat{\mathbf{k}})+\sum_{\mathbf{g}}R_{o\mathbf{g}}(\mathbf{k}_\parallel^{\rm inc})e^{i(\mathbf{K}_\mathbf{g}^--\mathbf{K}_o^+)\cdot(\mathbf{r}_a-\mathbf{r}_o)}\times f_a^+(\mathbf{K}_g^-\cdot\hat{\mathbf{k}})\ . \tag{23}$$

In Eqs. (20)–(23) we have used the notation of Wei and Tong,[13] in which the superscripts on the atomic scattering factors f indicate whether the scattering is *forward* (+, if the scattering angle $\theta<90°$) or *backward* (−, if $\theta>90°$). A problem with the use of the SWIFT kernel defined by Eqs. (21)–(23) is that the position $(\mathbf{r}_a-\mathbf{r}_o)$ of the adsorbate relative to the surface appears explicitly in the kernel. This is, of course, not known *a priori* and is one of the parameters sought. However, it will be noted from (22) and (23) that the quantity $(\mathbf{r}_a-\mathbf{r}_o)$ appears only in the arguments of complex exponentials, thus contributing only *phases* to the summations in (22) and (23). Given an initial total lack of knowledge of these phases, we follow the spirit of the maximum entropy principle[23] and choose the most *unbiased* distribution, namely, one of *random* phases. On this assumption, one may take

$$C\simeq\left[\sum_{\mathbf{g}}|R_{o\mathbf{g}}(\mathbf{k}_\parallel^{\rm inc})f_a^-(\mathbf{K}_\mathbf{g}^-\cdot\hat{\mathbf{r}})|^2\right]^{1/2} \tag{24}$$

and

$$D\simeq f_a^-(\mathbf{K}_o^+\cdot\hat{\mathbf{k}})+\left[\sum_{\mathbf{g}}|R_{o\mathbf{g}}(\mathbf{k}_\parallel^{\rm inc})f_a^+(\mathbf{K}_\mathbf{g}^-\cdot\hat{\mathbf{k}})|^2\right]^{1/2}\ . \tag{25}$$

It is well known that the angular variation of a typical atomic scattering factor is much greater in the *forward* than in the *backward* scattering direction for electrons of energies typically used in LEED. This is illustrated in Fig. 1, which depicts the variation with (polar) scattering angle of both the magnitude and the phase of the oxygen atomic scattering factor for electrons of energy $E=12$ hartrees (326 eV). Scattering angles close to zero correspond to forward-scattered electrons, while those close to 180° to backscattering. To a first approximation therefore, the backscattering factors in (21)–(23) may be taken as constant. On this approximation then, for a particular diffraction pattern, the term $f_s^-(\hat{\mathbf{r}}\cdot\mathbf{k})$ in (21) and the expression (24) for C may be regarded as constant. The first term of expression (25) for D may likewise be taken as constant. The second term in (25) contains the

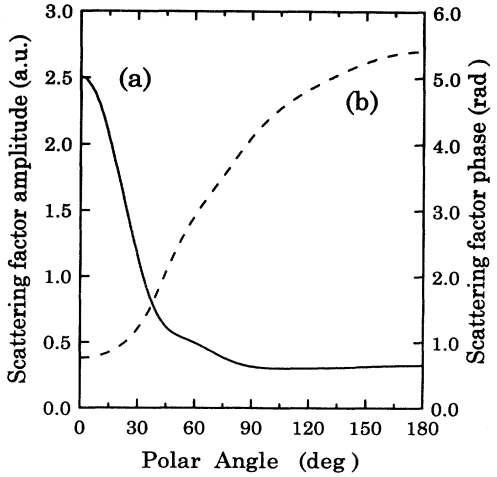

FIG. 1. Variation of (a) the magnitude (solid line) and (b) the phase (dashed line) of the atomic scattering factor of oxygen with angle of scattering (the abscissa).

forward-scattering factors $f_a^+(\mathbf{K}_g^- \cdot \hat{\mathbf{k}})$, each of which is peaked when $\hat{\mathbf{k}} \| \mathbf{K}_g^-$. However, since the second term consists of a sum over a range of Bragg-reflected wave vectors $\mathbf{K}_g^-$ whose directions cover essentially the whole of the backscattering hemisphere, we take the sum of the functions peaked at all those different directions as approximately isotropic.

Order-of-magnitude estimates of the quantities C and D may be made by approximating the backscattering factors by their values for 180° scattering, and the forward-scattering factors by their values for 0° scattering, and these estimates used to evaluate the kernel (21) for use in the reconstruction algorithm (16). Given the fact that atomic scattering factors vary more slowly with energy than scattering angle, however, we examine an even more drastic approximation, namely, we replace C and D by their averages $\langle C \rangle$ and $\langle D \rangle$, respectively, over all the available diffraction patterns.

Since in the resulting expression for the kernel (21), $f_s(\hat{\mathbf{r}} \cdot \mathbf{k})$ and $\langle D \rangle$ may be regarded as constants and thus act only as scaling factors, we may drop them from the kernel (21), which may then be written as[24]

$$K(k_\perp, \mathbf{k}_\parallel; \mathbf{r}) = \left[\frac{f_a(\mathbf{K}_o^+ \cdot \hat{\mathbf{r}}) + \langle C \rangle}{r} \right]^{-1} . \tag{26}$$

We found that, in practice, the quality of the reconstructed images remained good over quite a wide range of values assumed for $\langle C \rangle$. For the calculations reported in sec. IV, we took $\langle C \rangle = 1.5$ a.u., a quantity of the order of that estimated from (24).

We will show in what follows that, despite its remarkably simple appearance, the use of a kernel of the form (26) in the integrand of Eq. (16) enables the reconstruction of a high-quality three-dimensional image of the nearest-neighbor substrate atoms, even from a DLEED data set from electrons incident along a single direction onto the surface.

IV. THREE-DIMENSIONAL RECONSTRUCTION OF ADSORPTION SITES

In order to test our proposed algorithm, we simulated DLEED patterns from Ni(001) surfaces containing disordered layers of O atoms, adsorbed in the hollow, top, and bridge sites, respectively (see Fig. 2), using the computer program of Saldin and Pendry.[21] The DLEED patterns were calculated in each case for electrons, normally incident onto the surfaces, of 23 different energies, ranging from $E = 5$ hartrees ($\simeq 136$ eV) to $E = 16$ hartrees ($\simeq 435$ eV), in 0.5-hartree ($\simeq 13.6$-eV) intervals. The variation with electron energy of the DLEED patterns is illustrated in Fig. 3, which shows the simulated DLEED patterns at 9, 10, and 11 hartrees (245, 272, and 299 eV, respectively).

Our proposed reconstruction algorithm (16) with scattered-wave kernel (26) was applied to the series of diffraction patterns corresponding to each of the above adsorption sites in turn. The quantity $|B(\mathbf{r})|^2$ was calculated on a uniform three-dimensional (3D) voxel grid. The results for hollow-site adsorption are displayed in Fig. 4, those for the top-site in Fig. 5, and those for the bridge site in Fig. 6. The Cartesian axes x and y in these figures define a plane parallel to the surface, the z axes the outward surface normal. The origin of the coordinate system marks the position of the adsorbate atom in each case (represented by a sphere). The distance scales are

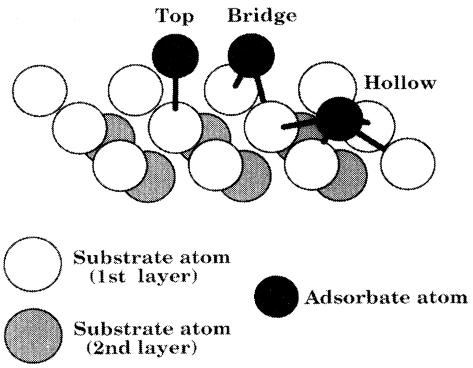

FIG. 2. Schematic diagram of the hollow, top, and bridge sites for atomic adsorption on a face-centered-cubic (001) surface.

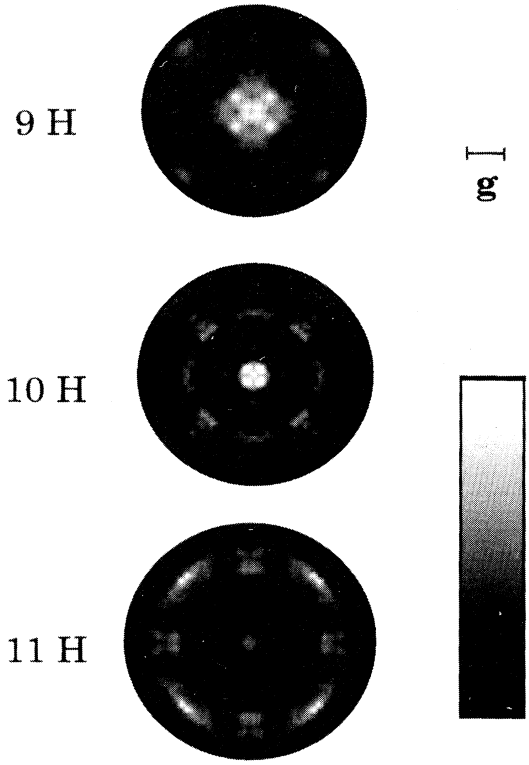

FIG. 3. Calculated diffuse LEED patterns from a lattice gas of oxygen atoms adsorbed on the hollow sites on a Ni(001) surface. The patterns due to normally incident electrons of three different energies, $E = 9$, 10, and 11 hartrees (245, 272, and 299 eV) are shown. The intensities are plotted on a uniform grid of $\mathbf{k}_\parallel$ values, and the magnitude and direction of a (10) reciprocal-lattice vector ($\mathbf{g}$) is also shown. The mapping of the gray scale to the intensities is indicated by the bar on the lower right.

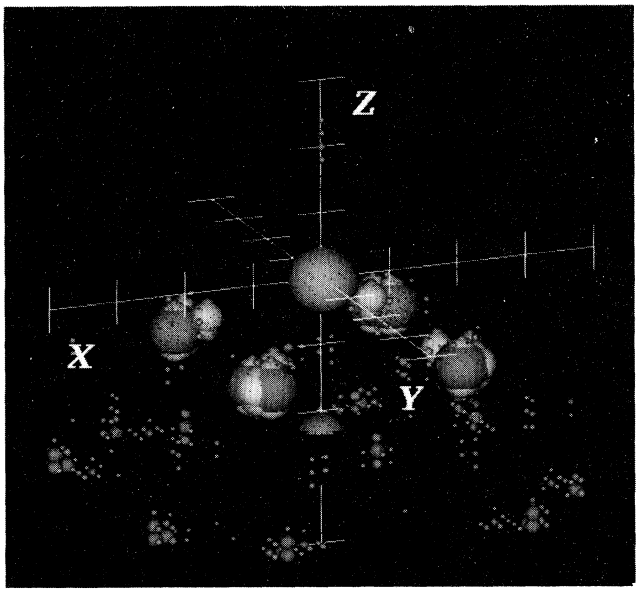

FIG. 4. Reconstructed image of the local atomic structure for hollow-site adsorption of oxygen on a Ni(001) surface. The adsorbed atom is at the origin of the 3D Cartesian coordinate system, and is represented by a sphere. The positions of the four nearest-neighbor Ni atoms in the outermost Ni layer, and that of the atom in the second Ni layer directly below the adsorbate are reproduced clearly.

specified by the ticks on the axes, at 1-Å intervals. The three-dimensional distributions are plotted in perspective, with the intensity at each voxel represented by a sphere whose radius is proportional to that intensity. The intensities were rounded to the nearest integer in the range 0–255 (single byte data), with 255 representing the maximum reconstructed intensity in the displayed cube. In order to eliminate the very low intensities, we imposed a threshold of 5% of the maximum below which intensities were not plotted.

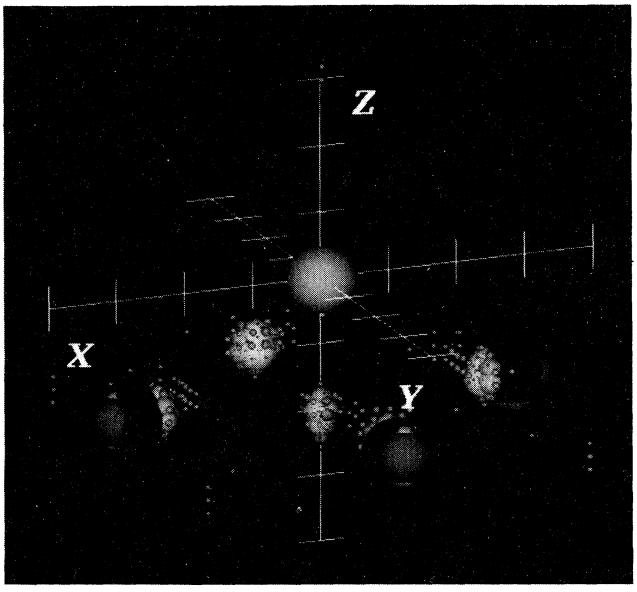

FIG. 5. Same as Fig. 3, except for top-site adsorption. Here the five nearest-neighbor atoms in the top Ni layer are reproduced.

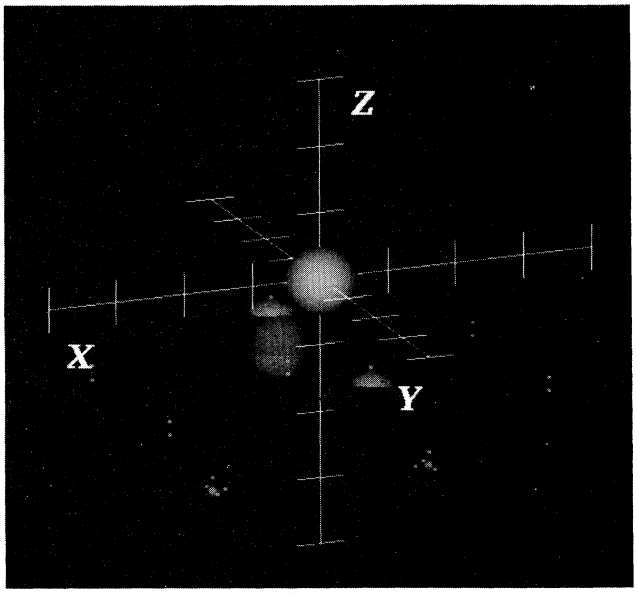

FIG. 6. Same as Fig. 3, except for bridge-site adsorption. Here the two nearest-neighbor atoms on the top Ni layer are reconstructed.

Remarkable fidelity is found on the reconstructed images, with high intensities at almost exactly the positions of the substrate atoms relative to the adsorbate for all three adsorption sites. Although the images presented in this paper (Figs. 4 to 6) were reconstructed from the 23 DLEED patterns referred to above, no noticeable degradation of image quality was found when the input data consisted of just 12 DLEED patterns at 1-hartree (27.2-eV) intervals in the same energy range.[25]

In a future paper we will discuss the accuracy with which the positions of the substrate atoms may be reconstructed. However, even a cursory examination of Figs. 3–5 indicates that the type of adsorption site, i.e., whether hollow, top, or bridge, is capable of being determined with graphic clarity. Although the nearest-neighbor atoms are reconstructed most obviously, some of the images, e.g., that of the bridge site in Fig. 6, also provide fainter indications of the positions of next-nearest-neighbor atoms.

The possibility also exists of using the information of the approximate positions of the adsorbate relative to the substrate apparent from Figs. 3–5 to calculate the quantities C and D from the exact expressions (22) and (23), respectively [rather than the approximate ones (24) and (25)], to get a better estimate of the kernel K to reconstruct a more accurate image. This process may be iterated for even more accurate results.

V. DISCUSSION

We comment here on the reasons that the technique presented here represents a significant advance over that

of Wei and Tong.[13] The first and obvious one is the elimination of the experimental requirement of measuring DLEED patterns from a variety of sample tilts (assuming a constant direction of electron beam incidence) in order to reconstruct a truly *three-dimensional* image.

The second is a little less obvious, and is related to an important point made in the original DLEED paper of Pendry and Saldin.[17] It was commented there that the assumption that the DLEED pattern, $H_{\rm calc}$, calculated for a model of a single adsorbate on a crystal surface, is identical (apart from a scale factor) to that, $H_{\rm exp}$, from an entire disordered layer of such adsorbates, is dependent upon *complete* lattice-gas disorder. Any residual ordering among the adsorbates would invalidate that assumption. In reality, the two quantities are related by

$$H_{\rm exp}=H_{\rm calc}S(\mathbf{k}_{\parallel}-\mathbf{k}_{\parallel}^{\rm inc}) , \tag{27}$$

where $S(\mathbf{k}_{\parallel}-\mathbf{k}_{\parallel}^{\rm inc})$ is a "structure factor" that characterizes the ordering among the adsorbates, and $\mathbf{k}_{\parallel}^{\rm inc}$ is the component of the wave vector of the incident electrons parallel to the surface. If the main object of interest is not this long-range order, but the local geometry of the adsorbate relative to the substrate, a device has to be found to extract $I_{\rm calc}$ from $I_{\rm exp}$. The solution proposed by Pendry and Saldin was the comparison between experiment and theory of not the bare intensities $H_{\rm exp}$ and $H_{\rm calc}$, but a quantity known as a Y function, constructed from the logarithmic derivative

$$Y(\mathbf{k}_{\parallel})=\frac{\delta H(\mathbf{k}_{\parallel})}{\delta E}\Big/H(\mathbf{k}_{\parallel}) \tag{28}$$

of the intensities with respect to electron energy at each value of $k_{\parallel}$ (for a given incident beam parallel wave vector, $\mathbf{k}_{\parallel}^{\rm inc}$). It is obvious from a comparison of (27) and (28) that a Y function calculated from $H_{\rm exp}$ would be identical to one from $H_{\rm calc}$, due to the cancellation in the quotient in (28) of the "structure-factor" term S.

It is clear from its definition (17) that the construction of the function χ also eliminates the "structure factor" S from measured DLEED intensities. Since our proposed reconstruction algorithm (16) operates on χ rather than on the bare intensities H, the reconstructed image will be quite insensitive to any residual long-range order due to interactions among the adsorbates. This probably has the important experimental consequence of enabling the short-range order of the adsorption site to be determined even at relatively high adsorbate coverages, when adsorbate-adsorbate interactions would be expected to be significant.

It should be noted that the method of construction of a similar signal-enhancing function χ by Wei and Tong[13] from derivatives of the DLEED intensities with respect to energy at a constant *direction*, $\hat{\mathbf{k}}$, of the detected wave vector does not have the desirable property of the complete elimination of the "structure factor" S. A further disadvantage of the need to combine data from diffraction patterns of several different electron energies corresponding to the same direction $\hat{\mathbf{k}}$ is that there is no way in general to prevent Bragg spots from passing close to a particular $\hat{\mathbf{k}}$ direction at *all* energies, whereas this is very easy to accomplish with a function of $\mathbf{k}_{\parallel}$. (The Bragg spots, of course, arise from scattering paths confined to the substrate, and are of no use for the determination of the *adsorbate* sites.)

In the case of an ordered adsorbate layer, superstructure Bragg spots are formed, in addition to those due to the substrate alone. Noting that[8,9] these may be regarded as sampling the DLEED intensities from the corresponding disordered adsorbate layer, and that all the Bragg spots occur at constant values of $\mathbf{k}_{\parallel}$, our algorithm would appear to be well suited for attempting holographic reconstruction in that case also. Indeed, in that case, the $\chi(k_{\perp},\mathbf{k}_{\parallel})$ function (17) may be constructed from data measured in conventional LEED, namely, the intensity versus energy (or I/E) variations of each of the superstructure Bragg spots.

VI. CONCLUSIONS

In this paper we have described a holographic computer algorithm that is able to reconstruct directly from a set of calculated diffuse LEED patterns arising from electron beams of a range of energies, incident along a *single* direction onto a surface consisting of a lattice gas of adsorbate atoms on a crystal substrate, a very accurate, and fully *three-dimensional* representation of the nearest-neighbor substate atoms. This is achieved by identifying a reasonable approximation to the anisotropy of the reference wave, and compensating for it. The particular algorithm that we propose also has the very desirable property of filtering out the effects on the DLEED patterns of any residual long-range order among the adsorbates. The DLEED patterns employed in our test calculations were performed by the established computer programs of Saldin and Pendry,[21] which have not only enabled surface structures to be found by conventional trial-and-error fits to experimental data, but have also paved the way for previous advances in holographic reconstruction algorithms. As such, we have little doubt that the technique will soon be able to reconstruct similar high-quality images of the local adsorption sites of atomic adsorbates from experimental data. The possibility that a similar algorithm may also be able to reconstruct directly the local adsorption sites of ordered adsorbates on surfaces from the I/E curves of superstructure Bragg spots is also noted.

ACKNOWLEDGMENTS

This work was supported by the National Science Foundation (Grant No. DMR-9320275) and by the Donors of the Petroleum Research Fund, administered by the American Chemical Society. D.K.S. is grateful to Professor J. B. Pendry, FRS for his hospitality at Imperial College, London during the latter stages of the writing of this manuscript, and to the United Kingdom Engineering and Physical Sciences Research Council for a Visiting Fellowship. X.C. acknowledges research fellowships from the Graduate School and the Laboratory for Surface Studies of the University of Wisconsin-Milwaukee.

[1]P. M. Marcus and D. W. Jepsen, Phys. Rev. Lett. **20**, 925 (1968); J. B. Pendry, *Low Energy Electron Diffraction* (Academic, London, 1974); M. A. Van Hove and S. Y. Tong, *Surface Crystallography by LEED* (Springer, Berlin, 1979); M. A. Van Hove, W. H. Weinberg, and C.-M. Chan, *Low Energy Electron Diffraction* (Springer-Verlag, Berlin, 1986).

[2]J. B. Pendry, K. Heinz, and W. Oed, Phys. Rev. Lett. **61**, 2953 (1988).

[3]J. B. Pendry and K. Heinz, Surf. Sci. **230**, 137 (1990).

[4]A. Szöke, in *Proceedings of the Topical Meeting on Short Wavelength Coherent Radiation: Generation and Applications, Monterey, CA, 1986,* edited by D. J. Attwood and J. Boker, AIP Conf. Proc. No. 147 (AIP, New York, 1986).

[5]J. J. Barton, Phys. Rev. Lett. **61**, 1356 (1988).

[6]D. Gabor, Nature (London) **161**, 777 (1948).

[7]D. K. Saldin and P. L. De Andres, Phys. Rev. Lett. **64**, 1270 (1990).

[8]M. A. Mendez, C. Gluck, and K. Heinz, J. Phys. Condens. Matter **4**, 999 (1992).

[9]P. Hu and D. A. King, Nature (London) **360**, 656 (1992).

[10]J. J. Barton and L. J.Terminello, in *The Structure of Surfaces III,* edited by S. Y. Tong *et al.* (Springer, Berlin, 1991); J. J. Barton, Phys. Rev. Lett. **67**, 3106 (1991).

[11]S. Y. Tong, H. Li, and H. Huang, Phys. Rev. Lett. **67**, 3102 (1991).

[12]L. J. Terminello, J. J. Barton, and D. A. Lapiano-Smith, Phys. Rev. Lett. **70**, 599 (1993); J. G. Tobin *et al., ibid.* **70**, 4150 (1993); H. Wu *et al., ibid.* **71**, 251 (1993); K.-M. Schindler *et al., ibid.* **71**, 2054 (1993); C. S. Fadley *et al.*, J. Electron Spectrosc. **68**, 19 (1994).

[13]C.-M. Wei and S. Y. Tong, Surf. Sci. **274**, L577 (1992).

[14]C.-M. Wei, S. Y. Tong, H. Wedler, M. A. Mendez, and K. Heinz, Phys. Rev. Lett. **72**, 2434 (1994).

[15]A. Szöke, Phys. Rev. B **47**, 14 044 (1993).

[16]D. K. Saldin, G. R. Harp, and B. P. Tonner, Phys. Rev. B **45**, 9629 (1992).

[17]J. B. Pendry and D. K. Saldin, Surf. Sci. **145**, 33 (1984).

[18]D. K. Saldin and J. B. Pendry, Comput. Phys. Commun. **46**, 129 (1987).

[19]B. P. Tonner, Z.-L. Han, G. R. Harp, and D. K. Saldin, Phys. Rev. B **43**, 14 423 (1991).

[20]D. K. Saldin, G. R. Harp, B.-L. Chen, and B. P. Tonner, Phys. Rev. B **44**, 2480 (1991).

[21]D. K. Saldin and J. B. Pendry, Comput. Phys. Commun. **42**, 399 (1986).

[22]K. Heinz, D. K. Saldin, and J. B. Pendry, Phys. Rev. Lett. **55**, 2312 (1985).

[23]*E. T. Jaynes: Papers on Probability, Statistics and Statistical Physics,* edited by R. D. Rosenkrantz (Kluwer Academic, Dordrecht, 1989).

[24]In subsequent work on diffuse LEED from K/Ni(001) [D. K. Saldin *et al.* (unpublished)], it was found that replacement of $f_a(\mathbf{K}_o^+\cdot\hat{\mathbf{r}})$ in (26) by its modulus, $|f_a(\mathbf{K}_o^+\cdot\hat{\mathbf{r}})|$, improved the quality of the reconstructed images.

[25]J. Vamvakas (private communication).

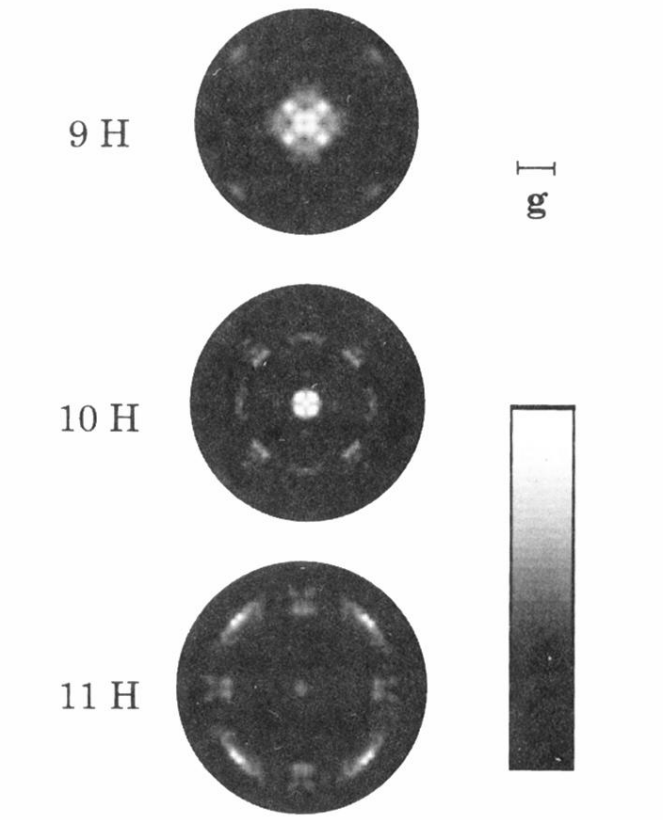

FIG. 3. Calculated diffuse LEED patterns from a lattice gas of oxygen atoms adsorbed on the hollow sites on a Ni(001) surface. The patterns due to normally incident electrons of three different energies, $E=9$, 10, and 11 hartrees (245, 272, and 299 eV) are shown. The intensities are plotted on a uniform grid of $\mathbf{k}_{\parallel}$ values, and the magnitude and direction of a (10) reciprocal-lattice vector ($\mathbf{g}$) is also shown. The mapping of the gray scale to the intensities is indicated by the bar on the lower right.

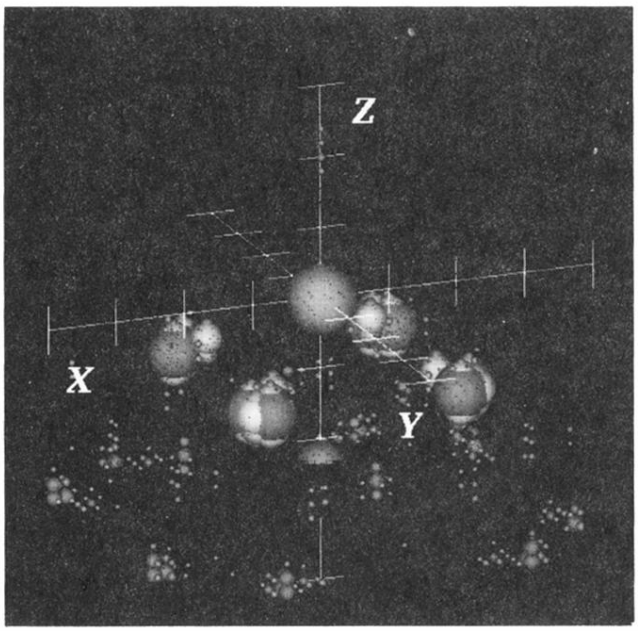

FIG. 4. Reconstructed image of the local atomic structure for hollow-site adsorption of oxygen on a Ni(001) surface. The adsorbed atom is at the origin of the 3D Cartesian coordinate system, and is represented by a sphere. The positions of the four nearest-neighbor Ni atoms in the outermost Ni layer, and that of the atom in the second Ni layer directly below the adsorbate are reproduced clearly.

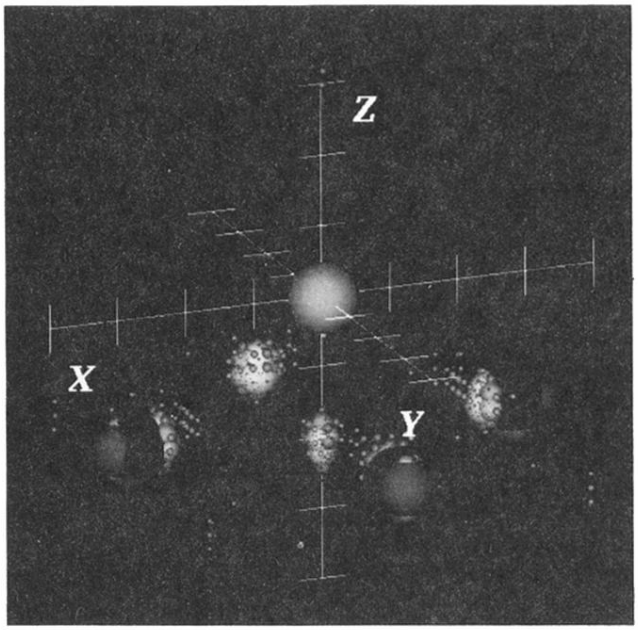

FIG. 5. Same as Fig. 3, except for top-site adsorption. Here the five nearest-neighbor atoms in the top Ni layer are reproduced.

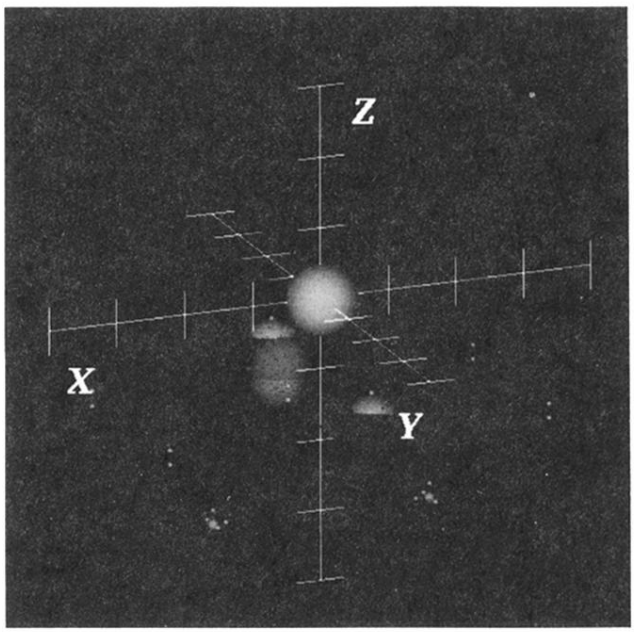

FIG. 6. Same as Fig. 3, except for bridge-site adsorption. Here the two nearest-neighbor atoms on the top Ni layer are reconstructed.